**Simulation of drag affecting synchronisers in a dual clutch transmission**

**Authors:** *Paul Walker[1], Nong Zhang[1], Ric Tamba[2], and Simon Fitzgerald[2]

[1]*Faculty of Engineering and IT, University of Technology, Sydney*
*15 Broadway, Ultimo, NSW, 2007, Australia*

[2]*NTC International*
*Unit F, 2 Hudson Avenue, Castle Hill, 2154, Australia*

**Mailing instructions:**

Paul Walker
C/O Professor Nong Zhang
University of Technology, Sydney
P. O. Box 123
Broadway, NSW 2007
Australia

Paul.D.Walker@eng.uts.edu.au

**Abstract:** The principle unknown in the actuation of synchroniser mechanisms is the drag torque acting on the mechanism. It has detrimental effects on the synchronisation time and energy, and influences the failure modes of this mechanism. In this paper a drag torque model for application to a synchroniser mechanism as used in dual clutch transmissions (DCT) has been developed. This includes torsional resistances from bearings, gear windage and friction, viscous shear in the concentrically aligned shafts and the wet clutch pack. Component resistances are amalgamated to a single torque that is employed on simulation of a synchroniser model in Matlab®. Simulations of the model are then run for typical up shifts, down shifts, and temperature variation. These results demonstrate that the DCT architecture has altered the impact of drag on the synchroniser mechanism, particularly with the influence of increased peak drag and the decoupling of drag torque from the type of shift.

**Keywords:** Synchroniser, Drag Torque, Numerical Simulation

## 1. Introduction

The process of synchronisation in manual (MT) and dual clutch transmission (DCT) systems is governed by torque generated at the cone clutch, blocking chamfers and through the losses generated in the target transmission components. Both the cone and blocking torques that are generated during synchronisation are well understood from the design and analysis perspective, and are controlled during the design process through selection of friction coefficient, operating diameters, and cone and chamfer angles [23, 16]. Drag torque, on the other, hand has a limited capacity for estimation as it is influenced by many variables that are not easily measurable or subject to a high degree of variation under standard operating conditions, tooth friction and the influence of electrohydrodynamic (EHL) lubrication being a typical example. To counteract this issue drag torque is typically estimated [16] in the design and selection phase of transmission development. Poor selection of drag torque will lead to the subsequent failure of the synchronisation process through several methods. Such failure modes include the block out of the sleeve such that ring unblocking cannot be performed, or to de-synchronisation of hub and sleeve prior to the indexing process being completed or to extended slip times of the cone clutch which results in damage to the friction surfaces.

Briefly, the conventional DCT comprises of synchronisers and gears that are found in manual transmissions (MT), but with clutches, and particularly clutch control, that is derived from automatic transmission (AT) technology. In this sense, the DCT can achieve fuel efficiencies of a MT while providing the simultaneous shifting capacity present in an AT. Conversely, with no AT torque converter, a significant damping source, the DCT is subject to torsional vibrations that would otherwise be damped out. Pointedly it can be expected that the MT has a unidirectional application of drag to the process as a result of coupling of gears, synchroniser and clutch, whilst DCT can be bidirectional depending on the speeds of engaged and target gears, particularly as the

open clutch speed is now decoupled from the target gear and fixed to the engaged gear speed.

Socin and Walters [23] and Razzacki [20, 21] present insight into the application of drag to the analysis of synchronisers, providing the equations and torque inequalities that govern asynchronisation and indexing phases of the process. Modelling and analysis of the process of synchronisation has been undertaken by [13, 17, and 18] with results targeting optimisation of the mechanism [13], or general actuation of the system [17, 18]. The results of [13] demonstrate clear variability of the indexing phase of the mechanisms actuation, where random alignment of indexing chamfers affects the duration of engagement. Lovas [18] includes a transmission model with the synchroniser which incorporates lubricant wiping of contact surfaces in the mechanism. However, overall consideration of drag effects is not discussed at length by these authors, where more comprehensive consideration may provide useful insight into failure phenomena of the mechanism.

Numerical analysis of drag torque on transmissions has been performed by Changenet [6] (helical) and Anderson [2] (spur), and on gear pairs by Heingartner and Mba [12], with the inclusion of successful experimental validation. Significantly [6] demonstrated the impact of temperature dependent variation of ATF properties on the accuracy of results, providing improvements of up to 10% when temperature dependent and independent models are compared. In both papers [12] and [6] consideration of bearing losses, gear windage and churning, and tooth friction are of primary consideration as sources of drag. These sources are responsible for the development of drag losses when shifting is excluded from the process. Further consideration of the layout of wet clutch DCTs suggests that during synchronisation viscous shear in the open clutch as well as shearing of concentric shafts must also be considered.

The development of this model is attempting to provide a good estimation of the drag torque generated during synchronisation, thereby revealing the impact of its variation on the process of synchronisation. The reality of the situation is that there is a degree of variability in drag through such factors as localised temperature changes, identified by Changenet [6] or impact of aging hydraulic fluid that will not be taken into account here. Primarily, as these inclusions will unnecessarily increase computational complexity without guaranteeing significant improvement of these results through simulation. Therefore, assumptions will be made about the temperature and lubricant to provide a reasonable simplification of these results to ensure an acceptable degree of precision is maintained.

The following sections of this paper are broken down into model formulation of the drag torque and synchroniser mechanism, where different sources of drag are discussed individually and brought together into a single drag torque model. The synchroniser mechanism is discussed briefly, including the influence of the DCT architecture on the process. This section is followed by simulations of drag torque experienced in the mechanism, comparing classical theory to this numerical model. As well as demonstrating a typical upshift and downshift, and finally shifting with the inclusion of the influence of temperature variation for normal shifts and cold starts.

## 2. Model Formulation

The dual clutch transmission comprises of helical gears and synchromesh synchronisers arranged on dual lay shafts, with concentrically aligned primary shafts are connected to the coupled multiplate wet dual clutch pack. To minimise the total drag in the system spray lubrication is used, eliminating higher drag from gear churning present in dip type lubrication, while maintaining sufficient lubricant over the gears. Drag torques are sourced at multiple points along a transmission and typically includes

windage and frictional bearing losses, tooth friction, gear windage or churning, viscous shear in the clutch and in the concentrically aligned shafts. Of these only frictional bearing losses and tooth friction losses are dependent on load, while the remaining losses are speed dependent.

FIGURE 1 HERE

Figure 1 presents a line diagram representing a typical wet clutch DCT. The synchronisers are green, bearings in red, and gears are labelled in blue. When synchronising a gear, G4 for example, the resistances of concern for the drag are only those present between the target synchroniser and the open clutch. In this instance losses are linked to the absolute velocity of components in the form of windage from gears 2, 4, and 6, and tooth friction from these same gears; as well as bearing losses from one bearing. There are also losses that are derived from the slipping speed between the locked and open clutches, the concentrically aligned shafts, and three bearings situated between these shafts. These losses must be calculated as point sources and then condensed into a single reflected drag torque acting at the synchroniser. This results in torque multiplication through the reduction gear pair.

During synchronisation when the vehicle is in motion one clutch is always engaged, and, as the two clutches are mechanically linked, the spacer plates will have the speed derived from the engaged gear. Conversely, the friction plates of the target gear will have a speed derived from the open synchroniser. As such, each target gear will have a different steady-state speed resulting from the drag torques on the mechanism. With two separate speed sources the drag torque is separated into absolute and relative drag modes each associated with the speed under consideration, the slipping speed of the clutch is perhaps the most significant change experienced by

the synchroniser as applied to the DCT and its effect has the potential to significantly affect the actuation of the mechanism as a whole.

## 2.1 Drag torques

### 2.1.1 Bearing Model

Bearing losses have been analysed by Harris [11] for a variety of bearing designs, considering both speed and load dependent losses on individual bearings. This work commonly considered to be the state-of-the-art on the topic, with similar results being applied through many other papers [6, 12]. Alternative bearing models are presented in [5] for radially and axially loaded bearings based on a bearing manufacturer's research. To maintain independence of this model from manufacturer specific information, [11] will be applied in this simulation. Equations for both windage and friction losses are provided below, along with the size of individual bearing used in the model. Load dependent bearing losses are:

$$C_L = f_L F d_m \qquad [1]$$

And speed dependent losses are:

$$\begin{aligned} &C_V = 10^3 f_V (\nu N)^{2/3} d^3 \\ &for\ \nu N > 2\times 10^{-3} m^2/s\min \\ &C_V = 16 f_V d^3 \\ &for\ \nu N < 2\times 10^{-3} m^2/s\min \end{aligned} \qquad [2]$$

### 2.1.2 Tooth Friction Model

Techniques used to model friction losses in gear teeth are dependent on both rolling and sliding friction [2, 13, and 24], modelling this friction coefficient has become quiet popular for both spur and helical gears. The majority of work investigates the friction force variation over the line of action of a single mesh, which must consider

involute geometry and vector analysis of contact forces. Other modelling methods consider more simple assessment of the losses that lead to more compact and efficient models that are more applicable to transient simulations.

Early work in Anderson and Loewenthal [2] requires the numerical integration of instantaneous rolling and sliding velocities along the path of contact, this must be divided into separate regimes depending on contact point of the meshed tooth. This method incorporates load sharing between teeth and divides the line of contact into shared and single tooth contact regions. Michlin and Myunster [19] provide an example of vector analysis of the contact topography of two teeth in mesh. The line of action of the mesh is divided into four zones relative to the pitch point. From this parameter equations are varied to account for vector changes, and friction load at different stages can then be calculated. Methods similar to those described by [2] and [19] become quiet cumbersome for modelling the time dependent variation of losses over multiple gears for an extended period and are more useful when investigating the mesh itself.

Diab [8], while focusing on the assessment of friction coefficient, provides demonstration of the accuracy of the preceding method, with the use of an appropriate friction coefficient the tooth friction force can be calculated accurately. Xu [24] reviews many of the current friction models and identifies a flaw in many friction models in that as the sliding velocity approaches zero at the pitch point the friction coefficient approaches infinity; this is a major issue with most current models as it create numerical issues. Electro-hydro dynamic lubrication (EHL) is identified as the most suitable method for developing friction models by [24] though it is not practical in terms of computational requirements and multiple parameter studies. EHL simulations were instead used by Xu [24] to develop a new friction model, with linear regression analysis giving a coefficient of determination of 94%. Like all friction models this is limited by the lubricant used in the simulation and experimentation.

An alternative friction model is presented by [4] and popularised in [6] and [8]. This model is an empirical correlation of fluid properties with gear speed and load, and as previously discussed has the disadvantage of tending to infinity at the pitch point. A significant part of both of these models is that both [4, 24] include rolling and sliding velocities in the model. This is required for accurate determination of the friction coefficient; however, as with the discussion of Anderson, etc. [2, 19] this requires precise calculation of tooth surface velocities, incorporating tooth geometry and relative alignment, thus such a method is still overly complex for this model.

To simplify this issue a constant friction coefficient will be applied to the model based on the available literature on gear tooth friction, this will reduce the computational complexity of the model while maintaining a reasonable degree of accuracy, particularly as the helical gear mesh results in multiple contact points over several gear teeth at any instant, effectively an average loss will be determined. Such assumptions have been taken by Changenet, *et al*, [6], and [Xu] provides reasonable reference to an average friction coefficient.

The question then turns to identifying appropriate macro scale models of gear friction losses that are computationally efficient. Changenet, *et al*, [6] provides an initial method for the evaluation of tooth friction power losses, with an alternative presented in BS ISO/TR 14179-1:2001 [5]. Both of the presented equations are functions of input torque, gear geometry, and friction. However in each case the gear geometry is treated quiet differently. The model selected by Changenet, *et al*, [6] has helix angle in the denominator and other geometry, such as module, in the numerator. This is reversed for the BS/ISO model, and, as a result it would be expected that the two results that are produced are substantially different. The inclination is therefore to accept the equations adopted by Changenet, *et al*, that are proven to be applicable in [6], nevertheless the BS/ISO model [5] will be adopted over this model as the rigorous

analysis utilised in the development of the model will results in its inclusion in the drag torque model. Further, [12] has also demonstrated its acceptability to numerical modelling. Power losses are determined as hence, with the result divided by rotational speed to result in torque loss:

$$P_M = \frac{fTN\cos^2\beta}{9549M} \quad [3]$$

Where:

$$M = \frac{2\cos\alpha\left(H_s + H_t\right)}{{H_s}^2 + {H_t}^2} \quad [4]$$

$$H_s = \left(\gamma - 1\right)\left[\sqrt{\frac{{r_{o2}}^2}{{r_{w2}}^2} - \cos^2\alpha} - \sin\alpha\right] \quad [5]$$

$$H_t = \left(\frac{\gamma + 1}{\gamma}\right)\left[\sqrt{\frac{{r_{o1}}^2}{{r_{w1}}^2} - \cos^2\alpha} - \sin\alpha\right] \quad [6]$$

In the lay shaft arrangement for the transmission type all even and odd gear pairs are attached to a common shaft that is connected to the clutch pack. The load for an individual gear is then the acceleration of its attached freewheeler on the lay shaft. For the gear pair under synchronisation the load is considered the acceleration of all components between it and the clutch pack, giving a much higher inertia than the freewheeling gears. It is therefore possible to ignore the considerably smaller resistance of non-targeted freewheeling gears over that of the gear targeted for synchronisation.

### 2.1.3 Gear Windage Models

Gear windage is defined as the drag of a gear as is rotates in air or an air-oil mixture, whilst churning is the drag generated as a gear rotates in oil. Both forms of loss are exclusively speed dependent. Churning losses arise from the partial submersion

of a gear in lubricant, with the drag developed from viscous resistance of the fluid. The churning of gears through transmission fluid is consistent with dip-type lubrication of the gear train. To minimise the losses in the DCT spray-type lubrication is generally adopted, this is associated with windage drag alone, therefore churning losses will be excluded from the model.

Similar to the churning of the gear through lubricant modelling of gear windage in an air or air-oil mixture is based on experimentation involving discs or drums rotating in this mixture, [22] examines this work. A review into the effects of windage power losses was conducted by Eastwick, *et al*, [10] who seeks to provide designers with the most appropriate information for the development of high efficiency gearboxes. Significantly, it is identified that the literature tends to utilise the same experimental apparatus to validate models as used to develop the same model. Thus "successful" results must be considered with some scepticism, as there is a lack of independence in the validation of results. Simulation by Al-Shibl [1] applies CDF techniques to the question of windage power losses to determine the ability to practically model this form of loss. Though it was possible to model these losses with reasonable accuracy there was a propensity for models to underestimate the windage at high speeds.

Anderson and Loewenthal [2] provide an initial model for the windage of gear-pinion pairs, using gear geometry, speed, and viscosity to correlate experimental data. Dawson [7] provides a second empirical model based on experiments that measure the deceleration of gears. Results were gathered for a varied range of gear parameters; however only air is used as the working fluid, and therefore the extent of impact of oil vapour is unknown. Dawson also [7] describes the formula presented as only being approximate, with insufficient data available based on the experiments performed to draw substantial conclusions. This literature, however, provides reasonable detail for comparison of model results.

Diab [9] provides two separate models for the windage of gears in air-oil mixtures. The first method is based on pi-theorem, as performed in the previous models of [2, 7], considers a combination of viscosity, speed, and geometry in developing a model. The second method applies fluid flow analysis in developing separate equations for faces, using friction force generated on the "disc" face, and teeth, where fluid flow is deflected by the proceeding tooth onto next tooth, generating a resistance force. This has the advantage of being independent of correlation using experimental equipment. Diab, *et al*, [9] demonstrates good comparison of both of these two methods, using a smaller quantity of experiments than [7] for example. However, as is suggested, the independence of the second method from experimental data provides it with an increased degree of confidence. These equations are:

Faces:

$$C_f = 2.586\pi \frac{1}{\sqrt{\mathrm{Re}^*}}\left(\frac{R^*}{R}\right)^5 + \frac{0.178\pi}{4.6}\left[\frac{1}{\mathrm{Re}^{*0.2}} - \frac{1}{\mathrm{Re}^{*0.2}}\left(\frac{R^*}{R}\right)^5\right] \quad [7]$$

Teeth:

$$C_t = \xi \frac{Z}{4}\left(\frac{b}{r_p}\right)\left[1 + \frac{2(1+X_A)}{Z}\right]^4 (1-\cos\phi)(1+\cos\phi)^3 \quad [8]$$

Where:

$$\phi = \frac{\pi}{Z} - 2(inv\alpha_P - inv\alpha_A) \quad [9]$$

### 2.1.4 Clutch shear

In the open multiplate wet clutch pack a differential velocity will result in the generation of a viscous shearing torque that resists the direction of motion. The ideal case is a relatively simple problem, demonstrates by the work of Kitabayashi [15] that provides demonstration of the drag torque that is accurate in low speed ranges. It has

been demonstrated by Yaun [25] that this is not applicable at higher speeds, and provides an improved model that has reasonable accurate at both high and low speeds.

Yuan [25] has proposed a logic to explain the phenomenon of reduced drag at high speeds, where a reduced effective radius is developed from the interaction of surface tension, centrifugal force and mass conservation. At high speed, centrifugal force pushes lubricant out of between the clutch plates in rivulets and reduces the effective contact area; this is countered by capillary action which draws the ATF against centrifugal motion. Therefore the balancing of these two forces can be used to estimate a reduced outer radius.

The effective drag torque is calculated using:

$$C_{Cl} = 2\pi \int_{r_1}^{r_0} \frac{\mu \omega r^3}{h} \left(1 + 0.0012\,\mathrm{Re}_h^{0.94}\right) dr \qquad [10]$$

Where the characteristic Reynolds number is defined by:

$$\mathrm{Re}_h = \frac{\rho \omega r h}{\mu} \qquad [11]$$

To determine the revised outer clutch radius two turbulent flow coefficients are found:

$$f = \begin{cases} 0.885\,\mathrm{Re}_h^{-0.367} & \left(\mathrm{Re}_h \geq 500\right) \\ 0.09 & \left(\mathrm{Re}_h \leq 500\right) \end{cases} \qquad [12]$$

$$G_r = \frac{1}{12}\left(1 + 0.00069\,\mathrm{Re}_h^{0.95}\right) \qquad [13]$$

It is convenient to note here that through application of mass conservation principles equations 11 to 13 can be solved at the inner clutch radius, particularly as fluid is pumped from the inner to outer radius.

Yuan's [25] theoretical analysis continues with the solving of the Reynolds equations using centrifugal and surface tension forces, which is arranged in polynomial

form, with the roots being solutions to the effective outer radius, which is then used in equation 10 as the outer radius if less than the existing outer radius:

$$\frac{\rho\omega^2}{2}\left(f+\frac{1}{4}\right)r_o^2-\frac{\mu Q}{2\pi r_m h^3 G_r}r_o+\frac{\mu Q}{2\pi r_m h^3 G_r}r_i-\frac{2\pi\cos\theta}{h}-\frac{\rho\omega^2}{2}\left(f+\frac{1}{4}\right)r_i^2=0 \quad [14]$$

Aphale, *et al,* [3] provides an alternative solution to the Naiver-Stokes equations that are solved by [25], etc. and like Yuan assumes that the centrifugal forces play a significant role in the fluid flow in the clutch. However, at the same time, it is assumed that viscous forces do not play a significant role in the distribution of forces, these results in some limitations to the results that are presented. Thus the method proposed by [25] is used for modelling the clutch drag.

### 2.1.5 Concentric Shaft shear

Particular to the DCT is the arrangement of concentric shafts that connect the gear train to the clutches. The arrangement of rotating concentric shafts is presented in [22] as an example of Couette flow, or simple shear flow. It is represented thus:

$$T=4\pi\mu h\frac{r_1^2 r_2^2}{r_2^2-r_1^2}\omega \quad [15]$$

The application of this equation requires the assumption that there is a continuous flow of lubricant through the annular area. This is justified as there are bearings separating these shafts which must be lubricated at all times.

## 2.2 Lubricant Properties

In wet clutch type DCTs it is desirable to use automatic transmission fluid as it has properties that are more acceptable for application to wet clutch systems. Kemp and Linden experimentally determine all the ATF properties that are required herein [14]. It

is expedient to use these properties, in table 1, for simulation of the synchronisation process. Note that the results for surface tension are only available a high temperatures (>90°C) and as a result linear extrapolation has been applied to determine the low temperature results. This is a significant assumption to the results as the behaviour of surface tension of this particular AFT is not well established through variation of temperature.

TABLE 1 HERE

### 2.3 Model Application

The process of synchronisation can be considered as a multistep linear engagement process, highly dependent on sleeve locations and the balancing of torques generated in cone clutch, chamfers, and drag. Initially sleeve and target gear are considered to have different initial speeds and a cone clutch is used to match speeds. The basic process steps are:

I. Initial displacement, where sleeve moves from the initial position to contact with the ring and hub
II. Ring rotation, where torque generated in the cone rotates the ring to blocking position with the sleeve
III. Asynchronisation, dry friction in the cone clutch matches speed of target gear and sleeve. torque imbalance between cone and chamfers prevents continued sleeve displacement
IV. Ring unblocking, with components synchronised, the cone torque is reduced to drag and acceleration of the target gear. If this is less than chamfer torques the ring is rotated into a neutral positions by the sleeve as the sleeve moves forward to engage the indexing chamfers

V. Displacement to hub chamfers, the sleeve continues to move forward until contact with the hub chamfers. During the stage there is risk of low cone torque and high drag forcing the de-synchronisation of the target gear, resulting in clash of the chamfers

VI. Hub chamfer engagement, chamfered teeth on the gear hub and sleeve contact and the sleeve continues to slide over the chamfers until interlocking between the two chamfer sets enables torque transfer from sleeve to target gear.

The modelling of synchronisers is, as previously stated, highly dependent on the balancing of torques from blocking chamfers, cone clutch friction, and drag. These are represented in the following inequality that must hold true if speed synchronisation is to be completed correctly, and post synchronisation it must fail to ensure unblocking of the ring:

$$T_I \leq T_C \qquad [16]$$

For indexing to occur successfully a different inequality must hold true to ensure unlocking of the cone clutch:

$$T_I + T_D \geq \left|T_C\right| \qquad [17]$$

Initially, if the absolute drag torque is greater than that if the indexing torque alone the result will be chamfer block-out of the sleeve.

Indexing and cone torques can be readily estimated using the following two equations.

$$T_I = F_S r_I \frac{1 - \mu_I \tan(\zeta)}{\mu_I + \tan(\zeta)} \qquad [19]$$

$$T_C = \begin{cases} 4\pi\mu_C R_C^3 L \dfrac{\dot{\theta}_{syn}}{h} & X_S < 2 \\ \dfrac{\mu_C F_S R_C}{\sin\psi} & X_S \geq 2, \dot{\theta} \neq 0 \\ T_{DRAG} + I_{FW}\ddot{\theta}_{FW} & X_S \geq 2, \dot{\theta} = 0 \\ \dfrac{\mu_{C,S} F_S R_C}{\sin\psi} & X_S \geq 2, \dot{\theta} = 0, T_{DRAG} > T_{CONE} \end{cases} \quad [20]$$

Through the use of hydraulic actuation of the synchroniser sleeve the sleeve force (Fs) can be assumed to be relatively constant. Additionally the friction coefficient of the indexing chamfers is constant, and, at least from a design perspective, the cone dynamic friction coefficient can be assumed to constant [16]. With these two referencing torques now estimated as being constant throughout the process it is possible to draw a set of parameters for the synchroniser and gears to apply to a simplified synchroniser model. The basic properties of the geartrain and synchronisers for both third and fourth gear are as follows:

TABLE 2 & 3 HERE

The synchroniser model is then developed through a relatively simple rigid body analysis. The use of a complete vehicle model is somewhat cumbersome for this purpose and as the vehicle inertia is several orders of magnitude larger than the synchroniser components it is unlikely that the torque resulting form synchronisation will have any affect on vehicle speed. Thus it is possible to eliminate the greater vehicle dynamics from the model. At the same time it is possible to assume that the vehicle speed is relatively constant over the duration of synchronisation, and from this the speed of the engaged clutch is constant. With these two assumptions it is possible to

model the synchroniser components that are of interest alone. This is presented in the diagram below:

FIGURE 2 HERE

For the purpose of simulations both up and down shifts will be considered as the relation between torque and speed will produce different steady state initial conditions prior to engagement of the synchroniser. Additionally two separate shifts will be considered in detail to demonstrate the influence of different drag components, first a 3 to 4 upshift, then a 4 to 3 downshift.

## 2.4 Synchroniser Time and Energy

The determination of total asynchronisation time is considered to be highly important to the selection of synchroniser design parameters [23]. It is a function of reflect inertia, initial and final speed, and net torque on the target gear. It is defined by Socin and Walters [23] as:

$$t_s = \frac{(\omega_f - \omega_i)I}{T_C \pm T_{Drag}} \qquad [21]$$

This is similar for single and multi-cone synchronisers, however with multi-cone synchronisers there are several input cone torques, such that $T_C=T_{C1}+T_{C2}+T_{C3}$.

Synchroniser energy calculations are based on the kinetic energy change resulting from synchronising, and the net energy required overcoming drag loss. Socin and Walters [23] define it as:

$$KE_s = \frac{(\omega_f - \omega_i)^2 I}{2} \pm E_{DRAG} \qquad [22]$$

$$E_{DRAG} = \int T_{DRAG} d\theta = (\omega_f - \omega_i) T_{DRAG} \cdot t_s \qquad [23]$$

In both equations [21 and 22] the "±" is applied based on shifting of the manual transmission, with upshifts being aided by drag and downshifts resisted by these losses. In the DCT this must now consider the speed change and direction of drag torque, with an upshift and for downshifts drag torque resists the asynchronisation of the synchroniser. This is a result primarily of the high clutch drag during the engagement process resisting all accelerations of the target gears from the steady state speeds.

Typically, without substantial knowledge of the acting drag torque on the mechanism it is accepted that a maximum drag torque is used as an approximate solution. Lechner [16] suggests that a reasonable approximation of torque loss is 2Nm is used as a design assumption for passenger vehicles.

Below the initial and final speeds of the target gears are presented for synchronisation. In each instance the speed of the sleeve is held constant at 1500RPM. Given that typical synchronisation duration is in the order of 20 to 100ms the variation in current gear speed is expected to be relatively small and this is therefore acceptable. Initial and final speeds are taken by running the simulation at steady before and after asynchronisation.

## 3. Results and Discussion

The evaluation of drag torque on the process of synchronisation requires significant appreciation of the interaction between acceleration of the target gear to synchronisation speed and said torque. The use of equations 21 to 23 for the estimation of synchronisation time and energy generated in the cone clutch provide some insight into the interaction of the applied torques to the mechanism. As previously stated it is assumed that the drag torque resists all engagement of the mechanism. With the variation of drag over the duration of the synchronisation process the resulting synchronisation time and energy must be significantly influenced.

FIGURES 3 & 4 HERE

Figures 3 and 4 show a comparison of the upshift and downshift asynchronisation time and energy, respectively. These results suggest that the numerical determination of synchronisation time thorough simulation demonstrates very reasonable agreement with the classical theory presented. However these results consistently underestimate the theoretical results. This is most predominantly a result of the ability to evaluate the variation of drag torque over the synchronisation process.

FIGURE 5 HERE

The comparison of assumed drag torque with numerically calculated drag demonstrates this variation, which will affect classical and numerical results. Downshift simulations in particular consistently overestimate the mean assumed drag. Resulting from the mechanism having drag based on the absolute gear speed and clutch slipping speed, where the relative motion of the clutch provides drag in the opposite direction to that generated from gearing. Thence opposite acting sources of drag reduce the overall drag torque.

FIGURES 6 & 7 HERE

Comparison of drag torque developed for different upshifts and downshifts demonstrates the significance of torque multiplication developed in the gear ratio, and the influence of fixed speed of the engaged gear. Most notably the high speed differential between first and second gears results in the development of large drag torques from the open clutch. This is further exacerbated through the gear ratios of both

these gears, and, along with significant differential speeds, provides the reasoning for the employment of multi-cone synchronisers; reducing synchronisation time and provide sufficient torque density to the mechanism such that high reflected drag torque is overcome in short time frames.

To evaluate the impact that drag torque has on the overall synchronisation process separate simulations will be processed. These will be typical up and down shifts using midrange gears. The first simulation will be the synchronisation phase a 4 to 3 downshift for a DCT, the sleeve will be maintained at a nominal speed of 1500RPM and the target gear will be initiated at the steady state speed of 4400RPM.

FIGURE 8 HERE

Figure 8 (a) shows the relative speeds of the synchroniser during the engagement process, as well as sleeve displacement. The results indicate a speed matching phase of 20ms, whilst the unblocking and indexing phases have duration of approximately 20ms. As the cone clutch synchronises the gear and shaft speeds the clutch slip speed increases, increasing the drag torque experienced by the synchroniser. The increased torque results in the extension of the unblocking and indexing processes, as shown in Figure 8 (b). The extension of these two phases of engagement is highly dependent on the direction of unblocking and indexing torques, and changes in alignment will modify the duration of the process. Drag torques are broken down into constituents in Figure 9 below.

FIGURE 9 HERE

Figure 9 (a) presents the drag on the system arising from the absolute speed of gears and bearings. The most significant of these loads is the windage generated on the accelerating gears, second to this is the tooth friction torque generated in the being

synchronised. This torque is smaller that what might be expected in a transmission, however this is a result of the load acting on the teeth is associated with the drag and cone torque rather than total vehicle torque, which may produce much higher resistance. The windage drag results from combined gears in the train as they are all accelerated, and will generate significant torque. Also, note that the bearing load is insignificant and has minimal impact on simulation results.

In Figure 9 (b) are the drag torques as a result of the slipping speed in the clutch and shafts. The viscous shear in the clutch dominates the drags generated as a result of the slipping speeds. This is a typical for wet clutch transmissions as the multiplate clutch pack is very close together; separation of 0.1 to 0.2 mm is common. This drag in particular dominates drag torques and for this form of down shift in particular extends the engagement process.

FIGURE 10 HERE

The results in figure 10 demonstrate the speed matching for a 3 to 4 upshift, with the speed the sleeve being 1500RPM, and $4^{th}$ gear initially at 1300RPM. The process duration extends to 85ms total, with 55ms of this time for speed matching. As can be seen from figure 11 below the overall drag torque is not unidirectional, initially it aids synchronisation, but clutch speed reversal then resists engagement, extending the asynchronisation period. During steady state the clutch slip is negative to counter other losses and cone viscous shear in the synchroniser, which is then reversed as a result of the applied gear ratios and hence relative speeds of both synchroniser and clutch.

FIGURE 11 HERE

Figure 11a presents similar absolute drag torques to figure 9a, again dominated by high speed windage. The results in figure 11b present a different drag torque

generated from the clutch shear. In comparing figure 9 and 13 it was established that the slipping speed in the clutch is greater for the upshift than the downshift. This is the most significant variation, with the third gear using a double cone clutch to overcome higher drag loads experienced in upshifts from second gear, as shown in Figures 6 and 7, a fourth to third downshift will have significantly reduced asynchronisation time in comparison to a third to fourth upshift. Additionally, the unblocking and indexing stages are similar for both up and downshifts shown, as a result of similar geometries. With higher drag torque countering the more acute chamfer angle used in third gear, which is required to push trough the larger resistance experienced.

FIGURE 12 HERE

Figure 12 presents the variation in drag torque at different temperatures, identical simulation parameters are used as for the previous 4 to 3 downshift. At operating temperature of 40 and 60 degrees centigrade the synchroniser engagement process is completed successfully in less than 40ms, and a 0° the engagement increases significantly to almost 70ms. Note that sleeve engagement of the cone clutch increases as the film wiping progresses, along with asynchronisation, and indexing. The dominant variable that is influenced by the temperature variation is the viscosity of the ATF. Table 1 presented the different fluid parameters at the set operating temperatures of 0°C, 40°C, and 60°c, with the viscosity being an order of magnitude greater at zero degrees then when at forty of sixty degrees centigrade. This has a considerable effect on the shearing torques generated in the clutch in particular. With the high viscosity the target gear drag torque presents an inflection at 45ms in Figure 14, as a result of the very high drag desynchronising the mechanism. This result is useful in improving the indexing of the mechanism, but at high drag torques as experienced here leads to clash failures in the mechanism.

## 4. Conclusion

In this paper a model for the approximation of the drag torque affecting the synchroniser mechanism in a wet dual clutch transmission has been presented. These sources of drag include bearing windage and friction, gear tooth friction, gear windage, shear in concentrically aligned shafts as well as shear in the wet multi-plate clutch. The results of the simulation demonstrate that the multi-plate clutch is the largest source of drag in the mechanism; as a result it has significant influence on the engagement of the mechanism when applied to the DCT.

Comparisons of popular theory to numerical simulations have demonstrated good agreement with synchronisation time and energy, as well as mean drag torques. However, the use of the classical method underestimates peak drag torques and numerical simulations of the synchroniser engagement process demonstrate the variation of drag torque over the asynchronisation phase of the engagement. Furthermore these high drag torques have greatest effect on ring unblocking and indexing of the mechanism.

Consideration of the temperature effects on the AFT properties implies that the drag torque will be significantly higher at low temperature, increasing the likelihood of failure of the synchroniser mechanism. This is exacerbated by the architecture of the DCT resulting in clutch drag always resisting the synchronisation process. At low temperatures in particular this greatly extends the engagement of the mechanism, which has the potential to lead to ring overheating and persistent damage to friction surfaces.

In conclusion the application of wet multiplate clutches in conjunction with synchromesh-type synchronisers in the DCT has lead to the development of higher variation in drag torque. This presents the synchronisation process with new operating characteristics that have not been previously experienced in the application of this mechanism. Given the correct circumstances this can result in the failure of the

mechanism to engage correctly, and indeed lead to the long term damage of the critical components of the synchroniser.

## 5. References


1. **Al-Shibl, K., Simmons, K. and Eastwick, C. N.** Modelling windage power loss from an enclosed spur gear. *Proc Instn Mech Engrs: Part A J. Power and Energy,* 2007, **221**331-341.
2. **Anderson, N. E. and Loewenthal, S. H.** Spur Gear System Efficiency at Part and Full Load. *In the conference NASA Technical Paper 1622,* 1980,
3. **Aphale, C. R., Cho, J., Schultz, W. W., Ceccio, S. L., Yoshioka, T. and Hiraki, H.** Modelling and Parametric Study of Torque in Open Clutch Plates. *Transactions of the ASME,* 2006, **128** (April), 422-430.
4. **Benedict, G. H. and Kelley, B. W.** Instantaneous coefficients of gear tooth friction. *ASME Transactions,* 1961, 459-470.
5. **BS ISO/TR 14179-1:2001.** Gears - Thermal Capacity - Part 1: Rating gear drives with thermal equilibrium at 95°C sump temperature. 2001,
6. **Changenet, C., Oviedo-Marlot, X. and Velex, P.** Power loss predictions in geared transmissions using thermal networks-application to a six speed manual gearbox. *Transactions of the American Society of Mechanical Engineers,* 2006, **128**(May), 618-625.
7. **Dawson, P. H.** Windage loss in larger high speed gears. *Proc Instn Mech Engrs,* 1984, **198A**(1), 51-59.
8. **Diab, Y., Ville, F. and Velex, P.** Investigations on Power Losses in high speed gears. *Proc Instn Mech Engrs: Part J: J Engineering Tribology,* 2006, **220**191-198.

9. **Diab, Y., Ville, F., Velex, P. and Changenet, C.** Windage losses in high speed gears - preliminary experimental and theoretical results. *Journal of Mechanical Design,* 2004, **126**903-908.
10. **Eastwick, C. N. and Johnson, G.** Gear Windage: A Review. *Journal of Mechanical Design,* 2008, **130**(March),
11. **Harris, T. A.** Rolling Bearing Analysis. 1966, John Wiley and Sons, Inc., 1st edition.
12. **Heingartner, P. and Mba, D.** Determining Power Losses in Helical Gear Mesh. *Gear Technology,* 2005, 32-37.
13. **Hoshino, H.** Analysis on Synchronisation Mechanism of Transmission. *In the conference SAE Technical Paper,* 1999, 1999-01-0734
14. **Kemp, S. P. and Linden, J. L.** Physical and Chemical Properties of a Typical Automotive Transmission Fluid. Tulsa, Oklahoma, October 1990, Paper number: 902148
15. **Kitabayashi, H., Yu Li, C. and Hiraki, H.** Analysis of the various factors affecting drag torque in multiple plate wet clutches. *JSAE Technical Paper,* 2003, **2003-01-1973**
16. **Lechner, G. and Naunheimer, H.** Automotive Transmissions - Fundamentals, Selection, Design and Application. 1999, Springer-Verlag, 1st edition.
17. **Liu, Y. and Tseng, C.** Simulation and Analysis of Synchronisation and Engagement on Manual Transmission Gearbox. *Int. J. Vehicle Design,* 2007, **43**(1-4), 200-220.
18. **Lovas, L., Play, D., Marialigeti, J. and Rigal, J.** Mechanical Behaviour Simulation for Synchromesh Mechanism Improvements. *Proc Instn Mech Engrs Part D: J Automobile Engineering,* 2006, **220,** 919-945.

19. **Michlin, Y. and Myunster, V.** Determination of Power Losses in Gear Transmissions with rolling and sliding friction incorporated. *Mechanism and Machine Theory*, 2002, **37**167-174.

20. **Razzacki, S. T. and Hottenstein, J.** Synchroniser Design and Development for Dual Clutch Transmission (DCT). *In the conference SAE Technical Paper*, Detroit, MI, USA, April 2007, 2007, 2007-01-0114

21. **Razzacki, S. T.** Synchroniser Design: A Mathematical and Dimensional Treatise. *SAE Technical Paper*, 2004, **2004-01-1230**

22. **Schlichting, H.** Boundary layer theory. 1979, McGraw-Hill Classic, 7th Edition

23. **Socin, R. J. and Walters, L. K.** Manual Transmission Synchronizers. *SAE Technical Paper*, **680008**

24. **Xu, H., Kahraman, A., Anderson, N. E. and Maddock, D. G.** Prediction of mechanical efficiency of parallel-axis gear pairs. *Journal of Mechanical Design*, 2007, **129**(January), 58-68.

25. **Yuan, Y., Liu, E., Hill, J. and Zou, Q.** An Improved Hydrodynamic Model for Open Wet Transmission Clutches. *Journal of Fluids Engineering*, 2007, **129,** 333-337.

**Appendix 1 – Nomenclature**

b – Face width

C – Drag torque

d – Diameter

F – Normal force

f – Friction

Gr – Turbulent flow coefficient

h – Fluid spacing

H – Sliding ratio at the start of the approach

H – Sliding ratio at the end of the recess

I – Reflected inertia

K – load intensity

L – half cone generatrix

M – Mesh mechanical advantage

N – rotational speed (RPM)

P – Mesh power loss (kW)

Re – Reynolds number (* denotes critical Reynolds number)

r – Radius (* denotes radius at critical Reynolds number)

Q – Flow rate

T – Torque

Z – module

$\alpha$ – transverse operating pressure angle (degrees)

$\beta$ – operating helix angle (degrees)

$\gamma$ – gear ratio

$\nu$ – kinematic viscosity

$\mu$ – dynamic viscosity

ρ – density

ω – rotational velocity (rad/s)

ψ – cone angle

ζ – Chamfer angle

**Subscripts**

s – start of approach

S – Sleeve

D - Drag

t – end of approach

M – Mesh

m – mean

V – windage

l – Pinion

I – index

C – Cone

o2 – gear outside radius

w2 – gear operating pitch radius

o1 – pinion outside radius

w1 – pinion operating pitch radius

A – Tooth tip

P– Pitch point

## LIST OF FIGURES



## LIST OF TABLES

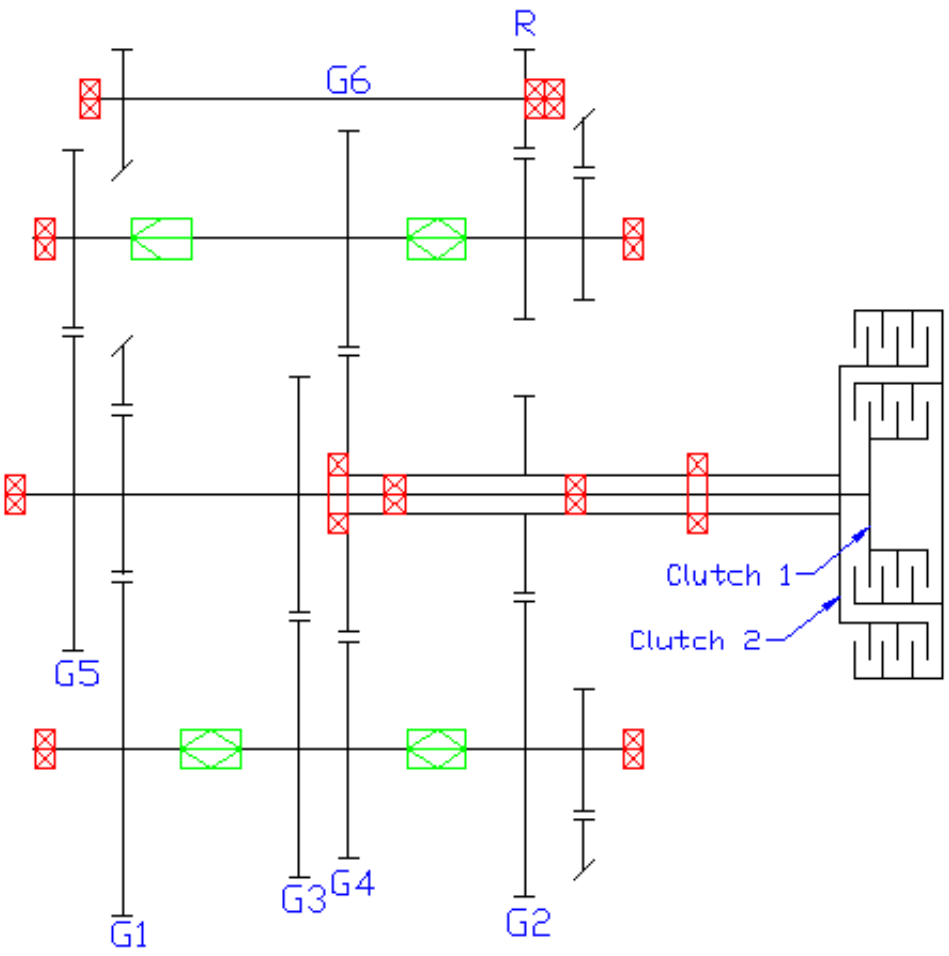


**Figure 13**

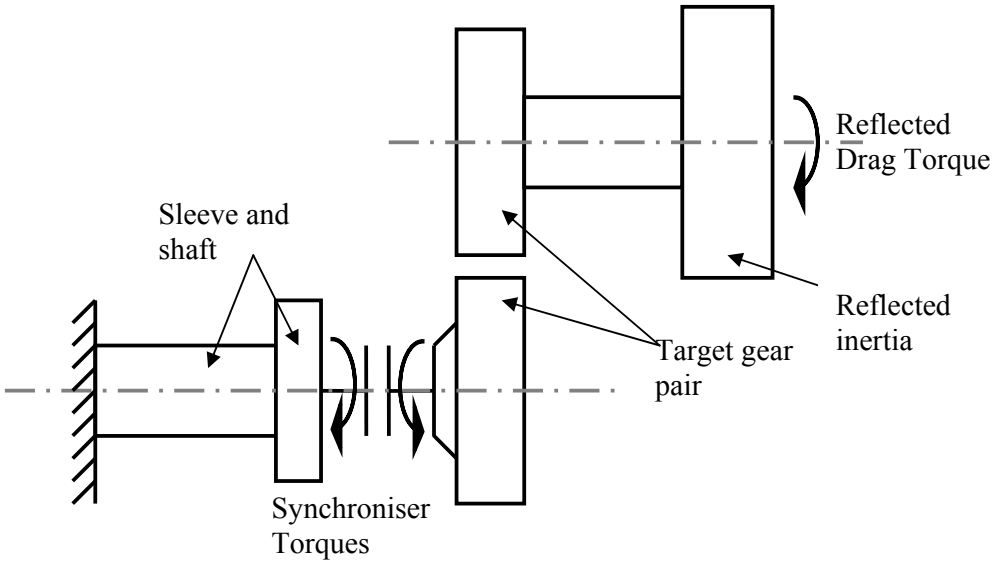
Reflected
Drag Torque
Sleeve and
shaft
Reflected
inertia
Target gear
pair
Synchroniser
Torques

**Figure 2**

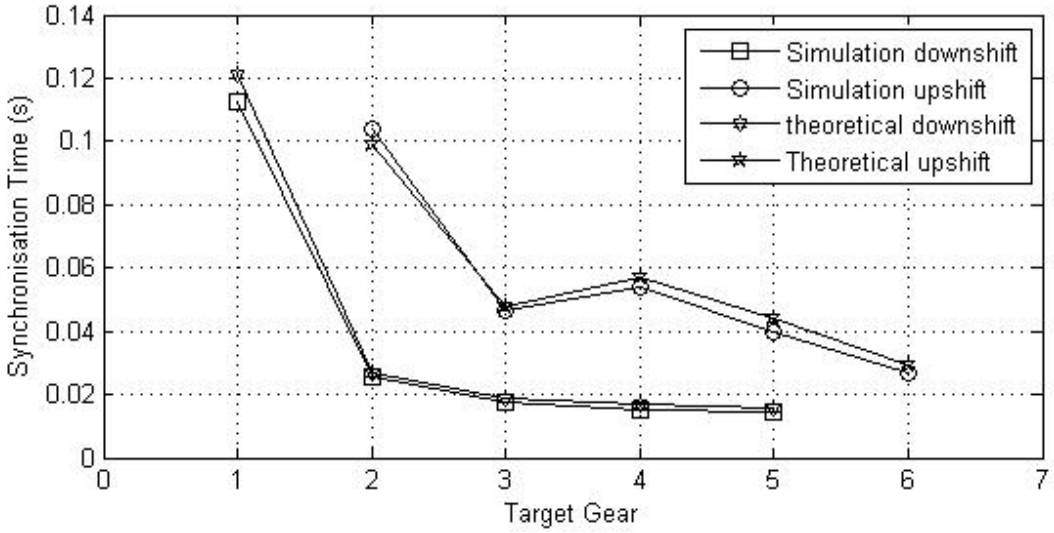
Synchronisation Time (s)
Target Gear
Simulation downshift
Simulation upshift
theoretical downshift
Theoretical upshift
0.14
0.12
0.1
0.08
0.06
0.04
0.02
0
0
1
2
3
4
5
6
7

**Figure 3**

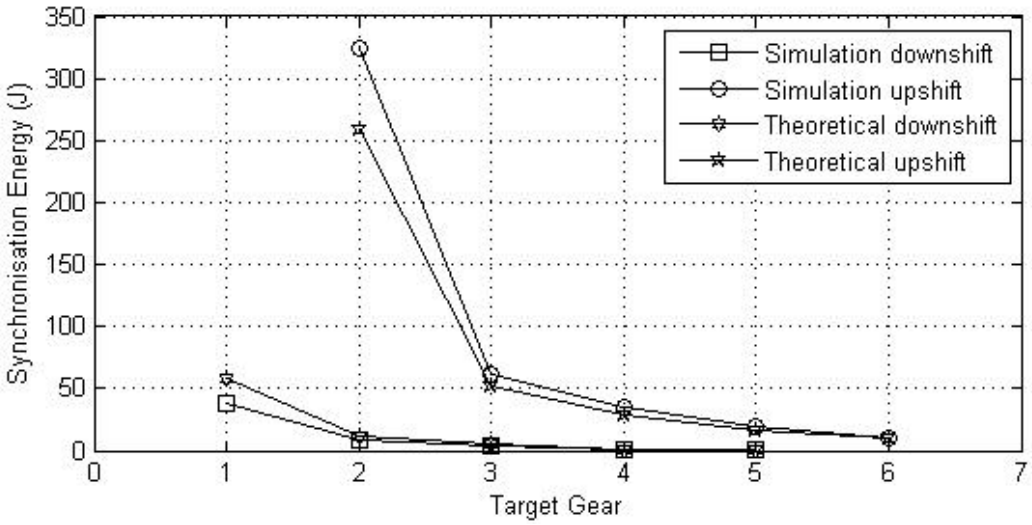
Synchronisation Energy (J)
Target Gear
Simulation downshift
Simulation upshift
Theoretical downshift
Theoretical upshift
0
50
100
150
200
250
300
350
0
1
2
3
4
5
6
7

**Figure 14**

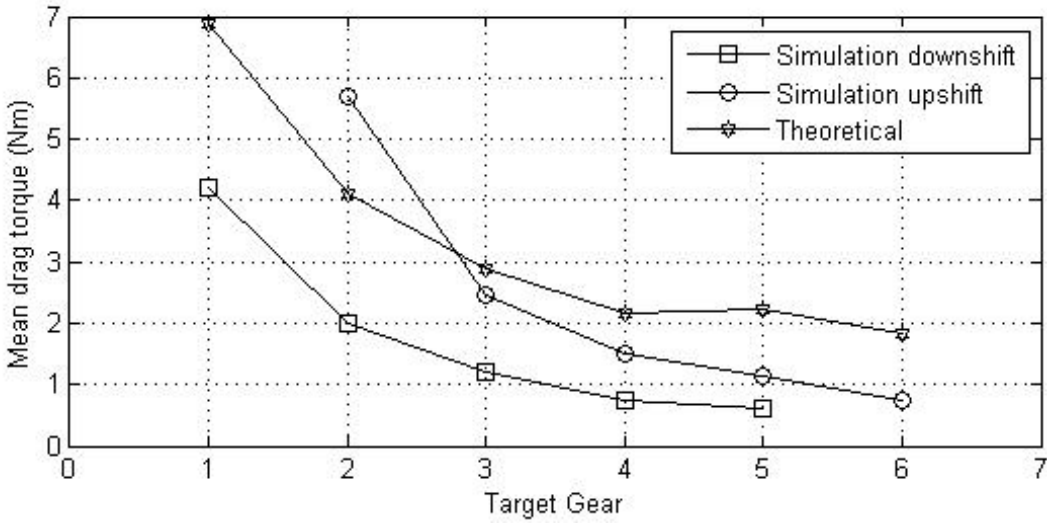
Simulation downshift
Simulation upshift
Theoretical
Mean drag torque (Nm)
Target Gear
0
1
2
3
4
5
6
7

**Figure 5**

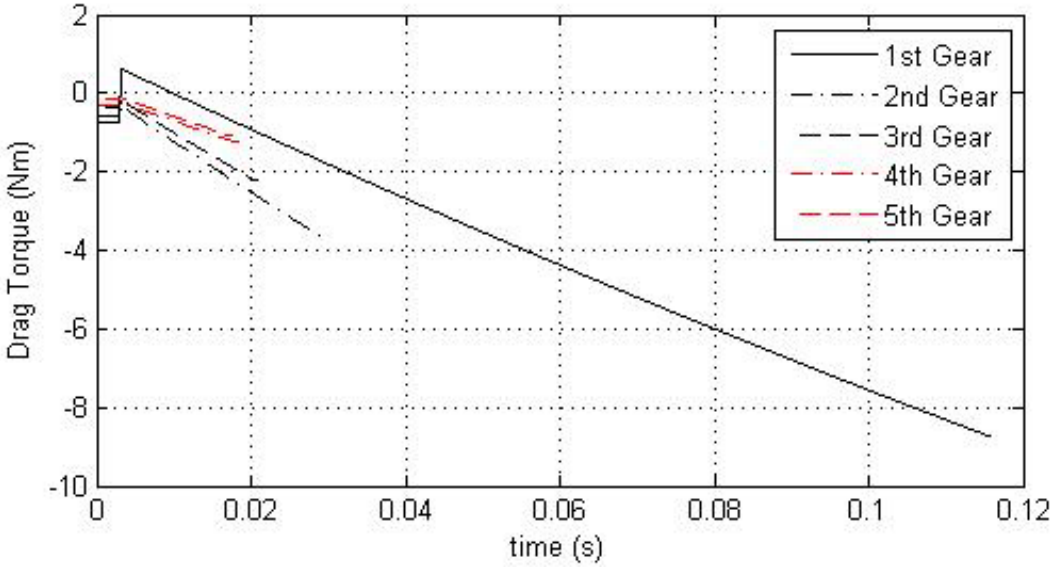
2
0
-2
-4
-6
-8
-10
Drag Torque (Nm)
0
0.02
0.04
0.06
0.08
0.1
0.12
time (s)
1st Gear
2nd Gear
3rd Gear
4th Gear
5th Gear

**Figure 6**

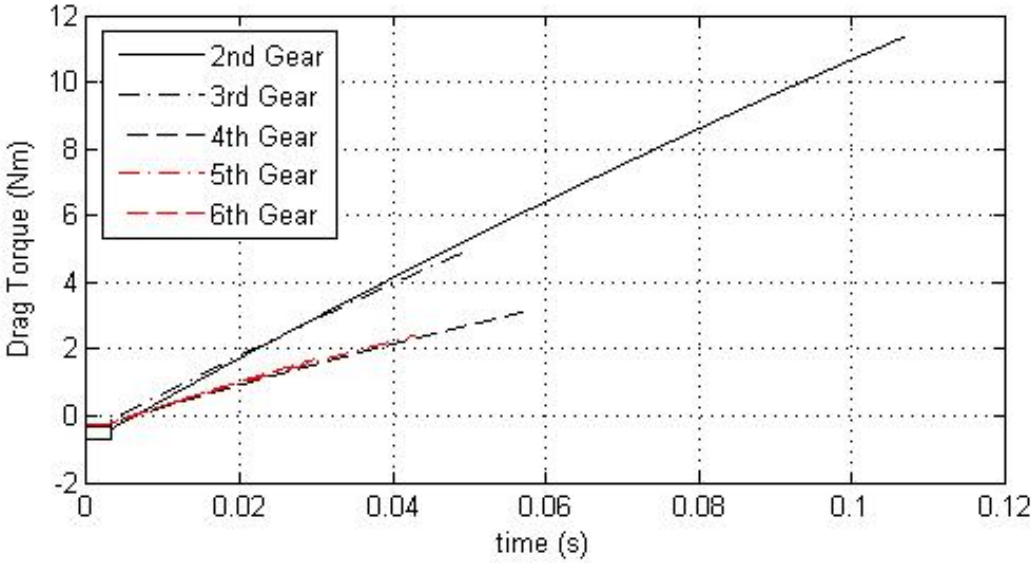
2nd Gear
3rd Gear
4th Gear
5th Gear
6th Gear
Drag Torque (Nm)
time (s)
12
10
8
6
4
2
0
-2
0
0.02
0.04
0.06
0.08
0.1
0.12

**Figure 7**

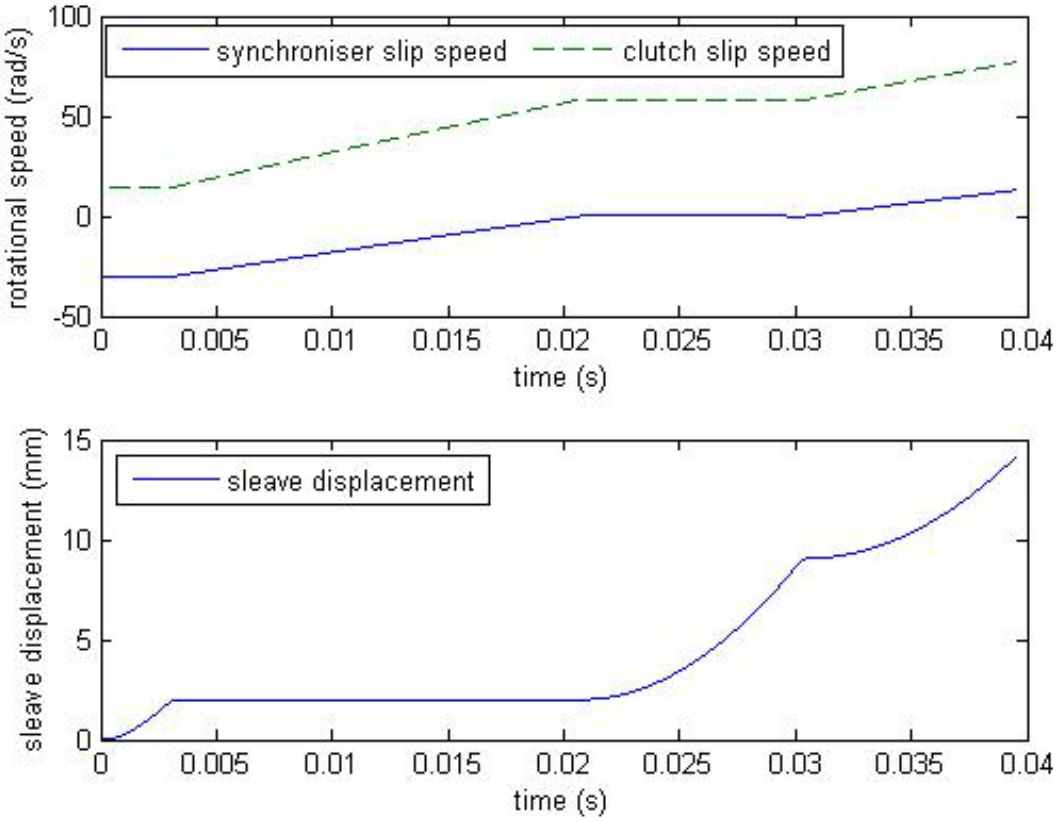


**Figure 8 a) and b)**

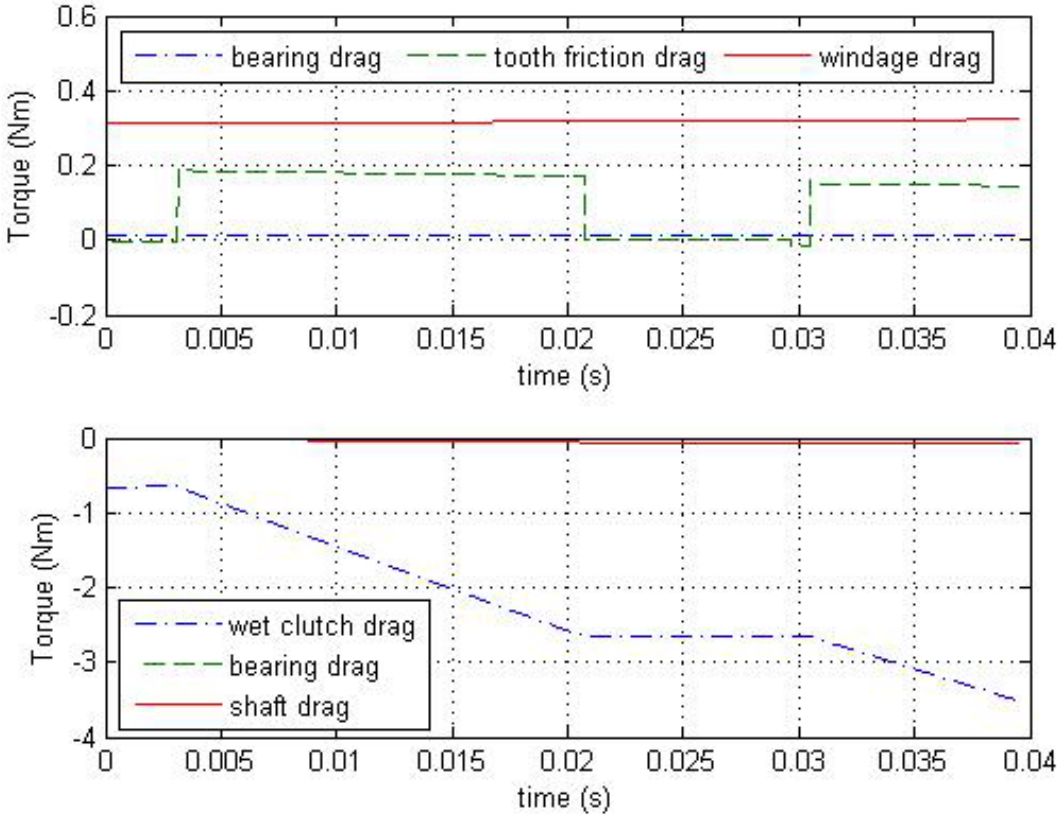


**Figure 9 a) and b)**

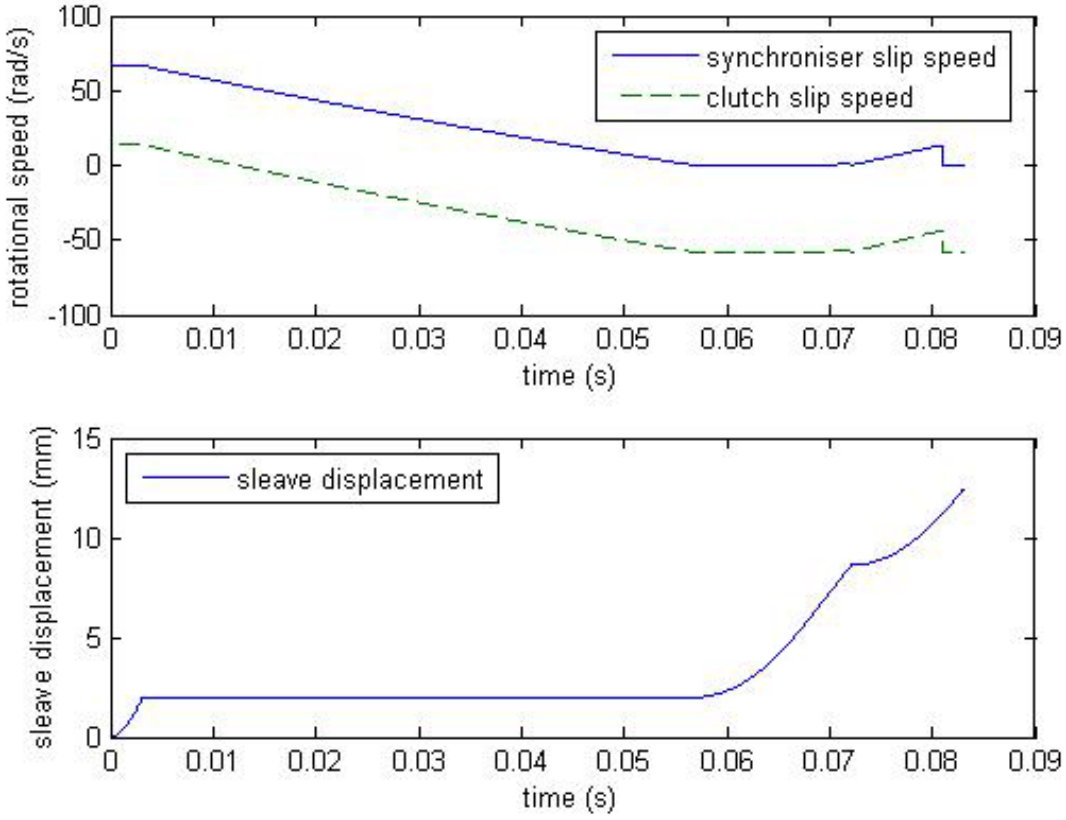


**Figure 10 a) and b)**

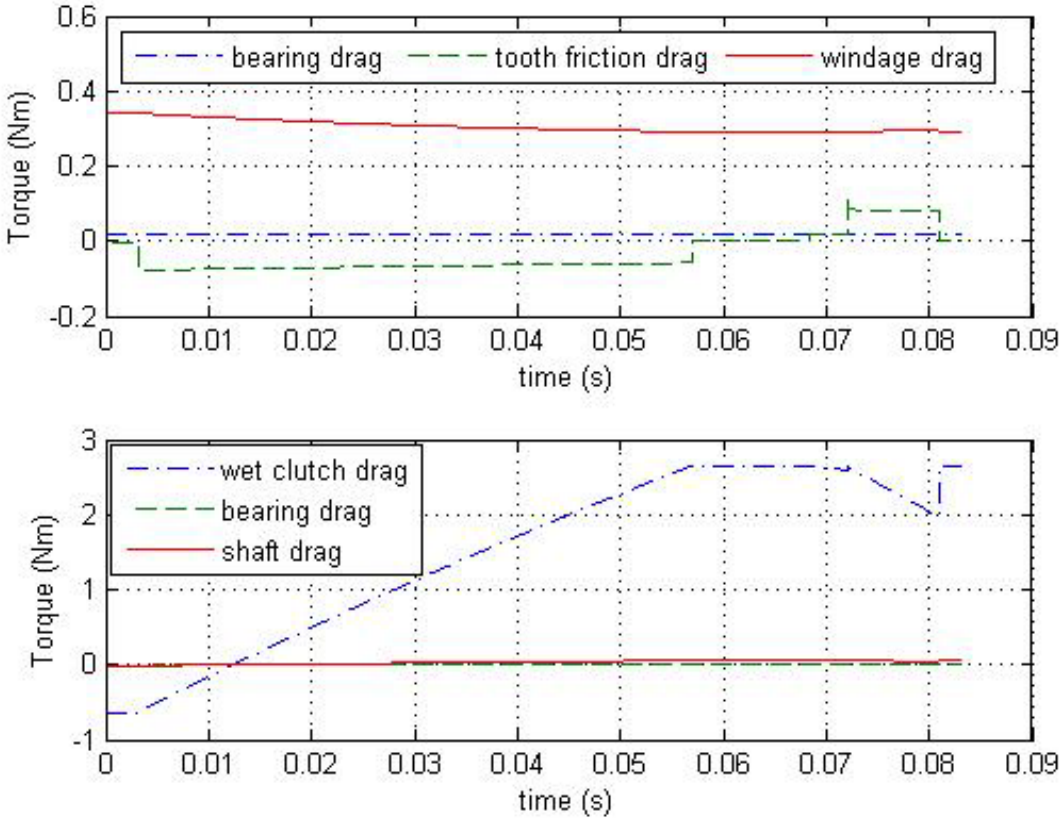


**Figure 11 a) and b)**

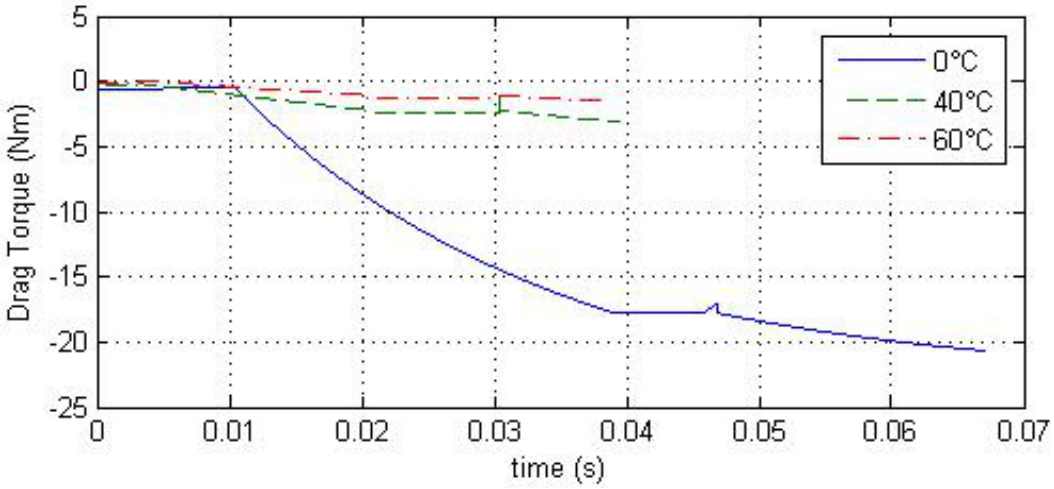
5
0
-5
-10
-15
-20
-25
Drag Torque (Nm)
0
0.01
0.02
0.03
0.04
0.05
0.06
0.07
time (s)
0°C
40°C
60°C

**Figure 12**

**Table 4**

| Temperature | 0°C | 40°C | 60°C |
|---|---|---|---|
| Density (kg/m3) | 881.2 | 853.4 | 839.4 |
| Viscosity (N.s/m) | 0.239 | 0.029 | 0.015 |
| Kinematic viscosity (m/s2) | $2.7 \times 10^{-4}$ | $3.4 \times 10^{-5}$ | $1.8 \times 10^{-5}$ |
| Surface tension (N/m) | 0.036 | 0.033 | 0.032 |

**Table 5**

| Gear | 1st | 2nd | 3rd | 4th | 5th | 6th |
|---|---|---|---|---|---|---|
| Gear ratio | 3.45 | 2.05 | 1.45 | 1.08 | 1.11 | 0.92 |
| Inertia of parts being synchronised ($kg \cdot m^2$) | 0.0714 | 0.0277 | 0.0143 | 0.0091 | 0.0092 | 0.0072 |

**Table 6**

| Gear | 1st | 2nd | 3rd | 4th | 5th | 6th |
|---|---|---|---|---|---|---|
| Number of cones | 3 | 3 | 2 | 1 | 1 | 1 |
| Mean cone diameter (mm) | 95 | | | | | |
| Cone angle (°) | 7 | | | | | |
| Cone friction coefficient | 0.1 | | | | | |
| Pitch diameter of chamfers (mm) | 120 | | | | | |
| Chamfer angle (°) | 35 | 35 | 35 | 55 | 55 | 55 |
| Chamfer friction coefficient | 0.1 | | | | | |